2019 IEEE Intelligent Vehicles Symposium (IV)
Paris, France. June 9-12, 2019

Reference Path Correction for Autonomous Ground Vehicles Driving Over Rough Terrain

Shaobo Wang, Pan Zhao, Yanghao Zheng, Biao Yu, Weixin Huang, Hui Zhu, Huawei Liang

***Abstract*—This paper proposes an online reference path correction algorithm for Autonomous Ground Vehicles (AGVs) driving in unstructured environments. Because the reference path which is not in accord with the road geometry cannot be directly executed by AGV, we use a correction baseline, which represents the road geometry, as the guidance to correct reference path. As the road geometry varies according to the road environment, we use the centerline of drivable area extracted with General Regression Neural Network (GRNN) or optimal path generated by multi-resolution local trajectory planner as the correction baseline to correct the distance and curvature errors of the reference path. The proposed algorithm is tested on our experimental autonomous vehicle in the realistic off-road scenarios. Experimental results demonstrated its capability and efficiency to reduce the search space of the local trajectory planner and improve the robustness of tracking the reference path.**

I. INTRODUCTION

Autonomous driving technologies have been a hot research topic for quite a long time, while its applications in unstructured environments such as rescuing, exploring and scouting remain challenging. The local trajectory planning plays a critical role in coping with these challenges. Related works on local trajectory planning can be categorized into two groups. One focuses on computing a long-term collision-free trajectory using heuristic search techniques or random graph-search algorithms [1][2][3]. These methods are too computationally demanding to deal with the higher dimensional state-space. Sampling-based trajectory planning algorithms have been proven to be very successful, which use a reference path to align the endpoints of local trajectory [4][5][6]. This technique reduces the search complexity and overcomes the danger of entering unsafe terminal states. The reference path is a main factor which determines the robustness and efficiency of the sampling-based local trajectory planner. However, in unstructured environments, only a finite number of task points through which the AGV must pass are given to approximate the reference path. Reference path generated with only task points contains considerable errors as shown in Fig. 1. Local trajectory planning with errors in reference path will cause instability of controlling the AGV [7]. Therefore, reference path correction in unstructured environments can significantly improve the robustness and the accuracy of local trajectory planner, which leads to better performance of tracking control.

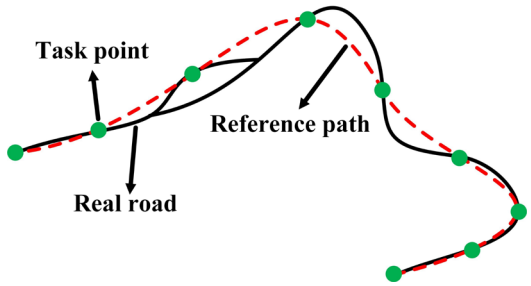

Fig. 1. reference path with error

II. RELATED WORK

A lot of works of reference path optimization have been proposed in structured environments. These methods usually use prior information such as digital map, lane line and road boundaries to approximate a smooth reference path, in which the curvature and derivative of the curvature are continuous, making the tracking control stable [8][9][10][11]. In unstructured environments, as the road geometry varies and prior information is insufficient. The reference path optimized with above methods may not accord with the road geometry when the reference path contain considerable errors, resulting in overshoot, oscillation or even require stop-steer-go motions [12][13]. Therefore, previous works that focus on path smoothing based on prior information are not suitable to correct the reference path online in unstructured environments.

In order to address the challenges in unstructured environments, we propose two different methods to generate the correction baseline which can represent the road geometry, and use the correction baseline to correct the reference path. The centerline extracted from the drivable area by GRNN, or

*Research supported from National Key Research and Development Program of China (Nos. 2016YFD0701401, 2017YFD0700303 and 2018YFD0700602),Youth Innovation Promotion Association of the Chinese Academy of Sciences (Grant No. 2017488), Research Program of Fire Bureau of Ministry of Public Security (Grant No. 2017XFGG04), Key Supported Project in the Thirteenth Five-year Plan of Hefei Institutes of Physical Science, Chinese Academy of Sciences(Grant No.KP-2017-35, KP-2017-13,KP-2019-16), Independent Research Project of Research Institute of Robotics and Intelligent Manufacturing Innovation, Chinese Academy of Sciences(Grant No. C2018005), and Technological Innovation Project for New Energy and Intelligent Networked Automobile Industry of Anhui Province.

Shaobo Wang and Weixin Huang are with the Institute of Applied Technology, Hefei Institutes of Physical Science, Chinese Academy of Sciences, Hefei 230031, Anhui, China and University of Science and Technology, Hefei 230026, Anhui, China.(e-mail: ba17168@mail.ustc.edu.cn, hwx2018@mail.ustc.edu.cn).

Pan Zhao, Biao Yu, Hui Zhu and Huawei Liang are with the Institute of Applied Technology, Hefei Institutes of Physical Science, Chinese Academy of Sciences, Hefei 230000, China. with Hefei Institution of Physical Science, Chinese Academy of Sciences and Anhui Engineering Laboratory for Intelligent Driving Technology and Application, Hefei, Anhui, China, 230031 (e-mail: pzhao@hfcas.ac.cn, byu@hfcas.ac.cn，hwliang@iim.ac.cn).

Yanghao Zheng is with the Shenzhen Key Laboratory of Advanced Communication and Information Processing, College of Information Engineering, Shenzhen University, Shenzhen 518000, China. (e-mail: 2172263012@email.szu.edu.cn;).

optimal path generated by multi-resolution local trajectory planner will be used as correction baseline depending on the road environments. Finally, the reference path will be corrected with correction baseline by offset correction and curvature correction.

The remainder of this paper is organized as follows. In Section III, we introduce the method of reference path initialization and method of vehicle localization on the reference path. Then, the correction baseline generation based on drivable area and multi-resolution local trajectory planner are described respectively. Finally, the method of using correction baseline to correct the initial reference path is presented in detail. Section V shows the experimental results in unstructured environments. Section VI concludes this paper.

III. Reference Path Correction Algorithm

In this section, we describe the proposed reference path correction algorithm in detail. An overview of the reference path correction algorithm is shown in Fig. 2. The reference path correction algorithm consists of the following three steps: Firstly, the initial reference path is approximated with the cubic spline. Then, the centerline of the drivable area extracted by GRNN method are used as correction baseline while the drivable area is reliable. Otherwise, the optimal path generated by multi-resolution local trajectory planner will be adopted as the correction baseline. Finally, the initial reference path is corrected by correction baseline using offset correction and curvature correction.

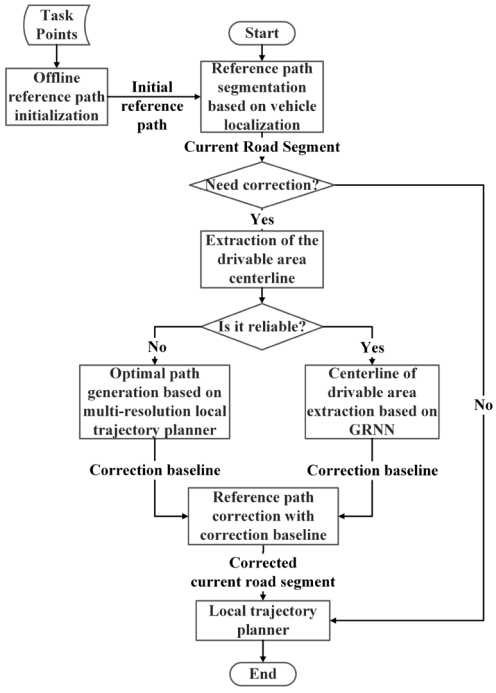

Fig. 2. Overview of reference path correction algorithm

A. Fitting the reference path with task points

The cubic spline provides the continuity of the second derivative. Therefore, the cubic spline is adopted as a representation of the initial reference path in this paper. The cubic spline consists of n cubic polynomial segments $S_i, i = 0,1,\cdots,n-1$, which connect the neighboring task points $[x_i, y_i]$ and $[x_{i+1}, y_{i+1}]$ with each other, and the determination of the curve segment S_i is defined by

$$S_i(x) = a_i + b_i(x - x_i) + c_i(x - x_i)^2 + d_i(x - x_i)^3 \quad (1)$$

with $i = 0,1,\cdots,n-1$. Due to the twice differentiability of the interpolation curve, within the transitions of the task points, the function values, the gradients and the second derivations have to match:

$$\left.\begin{aligned} S_i(x_i) &= y_i \\ S_i(x_{i+1}) &= S_{i+1}(x_{i+1}) \\ S_i'(x_{i+1}) &= S_{i+1}'(x_{i+1}) \\ S_i''(x_{i+1}) &= S_{i+1}''(x_{i+1}) \end{aligned}\right\}, \quad (2)$$

with $i = 0,1,\cdots,n-2$, and the boundary gradients are defined by the tangents in the starting point:

$$S_0'(x_0) = D_0 \quad (3)$$

where D_0 is the heading of the autonomous vehicle at the start point x_0.

B. Vehicle Localization on the initial reference path

As the car travels along the reference path, the reference path segment at which the vehicle is located can be determined by the closest point q_c on the reference path to the vehicle and heading h_c, as shown in Fig. 3. The current segment is bounded by two closest task points T_i and T_{i+1}.

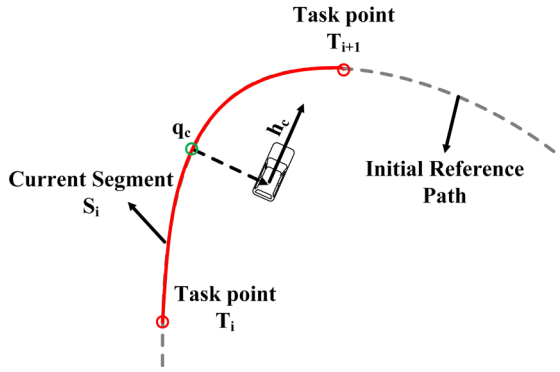

Fig. 3. Vehicle localization

C. Extracting the centerline of the drivable area

The drivable area, which is the free road surface ahead of autonomous ground vehicles, is computed from the laser data using a modified flood-fill algorithm [14]. The General Regression Neural Network (GRNN) is applied to extract the centerline from the drivable area since it can provide accurate and quick solution to approximation problem with noises in the inputs. GRNN is based on the following formula:

$$E(y|x_0) = \frac{\int_{-\infty}^{0} y f(x_0,y)dy}{\int_{-\infty}^{0} f(x_0,y)dy} \quad (4)$$

where $E(y|x_0)$ is the expected value of output; x is the estimator input vector; y is the output of the estimator, given the input vector x; $f(x_0,y)$ is joint probability density function of x and y.

A GRNN consists of four layers: input layer, pattern layer, summation layer and output layer. The transfer function from the input layer to the pattern layer is defined as (5).

$$\theta_i = exp\left[-\frac{(X-X_i)^T(X-X_i)}{2\sigma^2}\right] \quad i = 1,2,\cdots,n \tag{5}$$

where X is the input vector of predictor variables to GRNN, X_i is the specific training vector represented by pattern neuron i. In summation layer, the weighted summations of the outputs from the pattern neurons are used as follow shows:

$$S_S = \sum_i \theta_i \tag{6}$$

$$S_W = \sum_i \omega_I \theta_i \tag{7}$$

The GRNN output value y is estimated using the following equation:

$$y = \frac{S_S}{S_W} \tag{8}$$

In this paper, the centerline trained by GRNN can accurately represent the road geometry, as shown in Fig. 4. The black curve is the centerline of the drivable area which is shown as the green area.

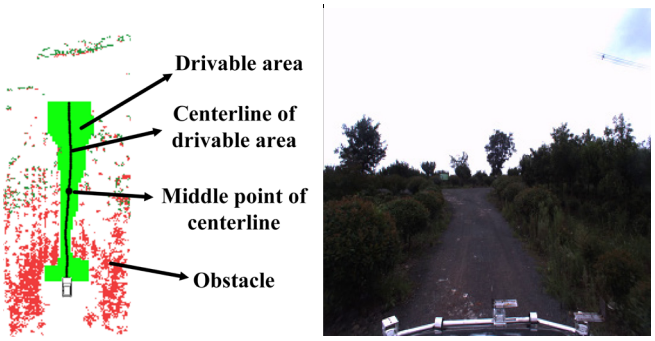

(a) (b)

Fig. 4. Centerline extraction based on GRNN. (a) a snapshot from the drivable area centerline extraction during field experiment. (b) the image taken by the front camera of the AGV.

D. Generating the optimal path based on multi-resolution trajectory planner

In unstructured environments, road surfaces such as earthquake-affected areas or forest floor, may be filled with obstacles. Therefore, the centerline of the drivable area is sometimes unreliable and cannot be used to correct the reference path, as shown in Fig. 5. The reliability of the centerline is evaluated by the length and the curvature change of the centerline. If the length of the centerline is greater than 30m, and curvature change compared with the last centerline is less than a specified threshold, the centerline of the drivable area is reliable. Otherwise, the centerline of the drivable area is regarded as unreliable and the optimal path generated by multi-resolution trajectory planner is used as correction baseline.

The multi-resolution trajectory planner is composed of state sampling, trajectory generation and evaluation. Firstly, the multi-resolution sampling strategy is developed to sample a set of terminal states in the control space. The terminal states are shown in Fig. 6 as the green circles. The sampling terminal states $X_F(\rho_f, \theta_f, \omega_f)$ is built from 3 layers of 39 points concentrated to the center, and the preview radius ρ_{min} should be greater than the minimal crash distance and smaller than the maximal perception distance, besides it could be a linear function of the current velocity as presented in (9). The sampling density could be modified by θ_f in order to produce bias trajectory candidates by exploiting the information on environmental structures.

$$\rho_{min} = \begin{cases} d_{min}, & f(v) < d_{min} \\ f(v), & otherwise \\ d_{max}, & f(v) > d_{max} \end{cases} \tag{9}$$

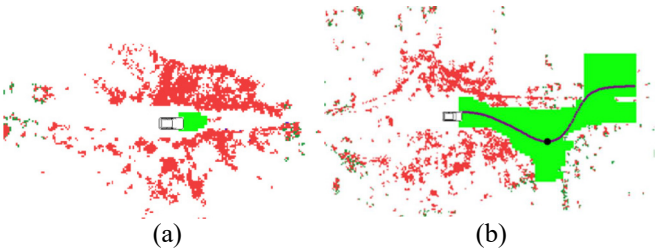

(a) (b)

Fig. 5. Illustration of unreliable drivable area. (a) obstacles on the road ahead. (b) a small road branched off to the right.

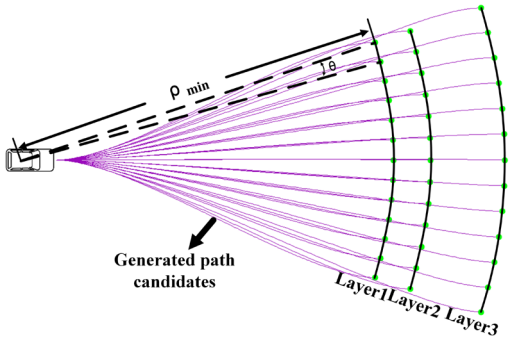

Fig. 6. Generation of path candidates

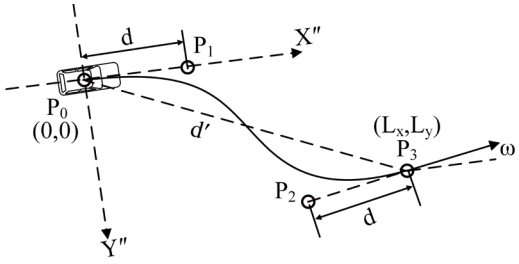

Fig. 7. A cubic Bezier curve with four control points

Once the terminal states have been determined, the cubic Bezier curve constructed by four control points is used to generate trajectories for every terminal state. The cubic Bezier curve are defined in (10).

$$C(t) = B_{0,3}(t)P_0 + B_{1,3}(t)P_1 + B_{2,3}(t)P_2 + B_{3,3}(t)P_3 \tag{10}$$

where $B_{i,3}$ is the Bernstein polynomial, as given by

$$B_{i,3}(t) = \binom{3}{i}\left(\frac{t_1-t}{t_1-t_0}\right)^{3-i}\left(\frac{t-t_0}{t_1-t_0}\right)^{i}, t \in \langle 0,1,2,3\rangle \tag{11}$$

As shown in Fig. 7, the coordinate system (X'', Y'') is built with the origin P_0 at the center of the vehicle, the vehicle's initial heading as the x axis. The terminal state will be the point P_3. P_1 is obtained by moving forward with distance d along the vehicle's initial heading from the start point. P_2 is obtained by moving backward with distance d along the

terminal heading from the point P_3. The position of the control points is defined by:

$$\mathrm{P}_0 = \begin{bmatrix}0\\0\end{bmatrix}, \mathrm{P}_1 = \begin{bmatrix}d\\0\end{bmatrix}, \mathrm{P}_2 = \begin{bmatrix}L_x - d\cos\omega\\ L_y - d\sin\omega\end{bmatrix}, P_3 = \begin{bmatrix}L_x\\L_y\end{bmatrix} \quad (12)$$

where L_x and L_y are lateral offset and the longitudinal offset of the terminal state P_3 to P_0. And ω is the angle between the terminal heading and the direction of the x axis. The terminal heading is defined as the tangential direction of the closet point on the reference path to P_3.

Equation (10) and (11) can be rewritten by applying (12). The Bezier curve is represented as:

$$\mathrm{x}(t) = (3d + 3d\cos\omega - 2L_x)t^3 - 3(2d + d\cos\omega - L_x)t^2 + 3dt$$

$$\mathrm{y}(t) = \left(3d\sin\omega - 2L_y\right)t^3 - 3\left(d\sin\omega - L_y\right)t^2 \quad (13)$$

Besides, the curvature of the generated path can be derived by applying (13) and (14).

$$\kappa(t) = \frac{x'(t)y''(t) - y'(t)x''(t)}{(x'(t)^2 + y'(t)^2)^{3/2}} \quad (14)$$

And the maximum of the curvature should satisfy the following condition to meet the vehicle nonholonomic constraint.

$$\kappa(t_m) \le \frac{\tan(\varphi_{max})}{L} \quad (15)$$

where L is the vehicle wheelbase, and φ_{max} is the maximum steering angle of the vehicle.

The maximum of the curvature $\kappa(t_m)$ is a function of d. The value of d that satisfies the above constraint can be found by brutal searching from $\frac{d'}{6}$ to $\frac{d'}{2}$, where $d'$is distance between P_0 and P_3. The processing time can be reduced by building a look up table that takes ω, L_x, L_y, d and returns maximum curvature of the Bezier curve. A group of path candidates are generated from all the terminal states.

Then, an obstacle cost function is introduced to evaluate the path candidates, as defined by (16).

$$\mathrm{J}_o(\tau_i) = \sum_{j=1}^{N} C(j)ds \quad (16)$$

where $C(j)$ denotes the distance to obstacles from the path candidate on the occupancy grid map, as represented in (16), d_{lat} is the lateral offset of the obstacle and the generated path τ_i , d_{lon} is the longitudinal offset of the obstacle to the vehicle. N is the number of cells of the grid map within 5 meters from the path τ_i. *M(j)* stands for the existence of obstacle in *j*th cell.

$$C(\tau(s)) = \begin{cases} \frac{1}{d_{lat}} * \frac{1}{d_{lon}}, & M(j) = 1 \\ 0, & M(j) = 0 \end{cases} \quad (17)$$

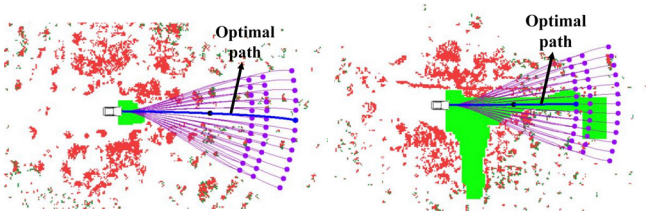

(a) (b)

Fig. 8. Optimal path generated by multi-resolution trajectory planner. (a) obstacles on the road ahead, (b) a small road branched off to the right.

The optimal path can be extracted from the path candidates by finding the path candidate that has lowest cost. As shown in Fig. 8, the optimal path can represent the road geometry and can be used as correction baseline.

E. Reference path correction

The reference path will be corrected in two ways, offset correction or curvature correction, depending on the offset d_c and angle θ between initial reference path and the correction baseline. As shown in Fig. 9, the offset d_c is determined by following formula:

$$d_c = x_1 - x_m \quad (18)$$

where (x_m, y_m) is the middle point of the correction baseline, (x_c, y_c) is the closest point on initial reference path to (x_m, y_m).

The angle θ is defined by the angle between the tangent lines of point (x_m, y_m) and (x_c, y_c).

If θ is greater than 10 degrees, the reference path will be corrected by curvature correction. Initially, the reference path segment is reconstructed by fitting a new cubic spline curve with the control points including the task points T_i and T_{i+1} bounding the segment, the center of the baseline M and the position of the vehicle V. Then, every time a baseline with θ greater than 10 degrees is generated, the corresponding point M and point V are treated as new control points. If distance from new control points to the last newly added control points are greater than 10m and horizontal distance difference is less than 1.0m, the new control points are added to the existing control points and a new curve is fitted. Otherwise the curve will stay the same.

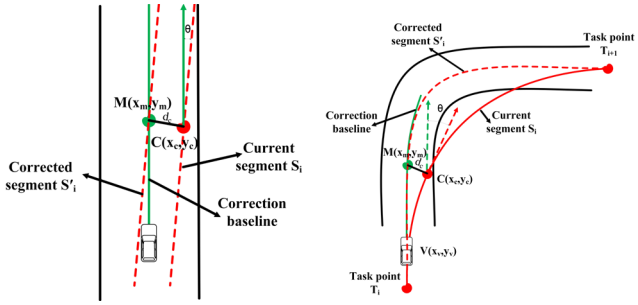

(a) (b)

Fig. 9. An example of the reference path correction method. (a) offset correction, (b) curvature correction

If θ is less than 10 degrees, the reference path will be corrected by offset correction, where the current segment S_i is shifted along the x axis:

$$\begin{cases} x_i' = x_i + \Delta s \\ y_i' = y_i \end{cases} \quad (19)$$

where Δs is defined by:

$$\Delta s = \begin{cases} d_c, & d_c \ge 1 \\ 0, & d_c < 1 \end{cases} \quad (20)$$

IV. Experimental Results

In order to test the performance of the proposed reference path correction algorithm, we conduct field tests in unstructured environments on our test autonomous vehicle, as shown in Fig. 10. Given the constraint that the distance between the adjacent task points are greater than 50m, 35 task points are randomly selected with Google Earth. The length of the reference path is 7.5 km. As shown in Fig. 11, the green curve describes the reference path generated with task points. It can be seen from Fig. 11 that the reference path contains considerable distance errors and curvature errors.

Fig. 10. Our autonomous vehicle test platform

Fig. 11. Task points provided by Google Earth

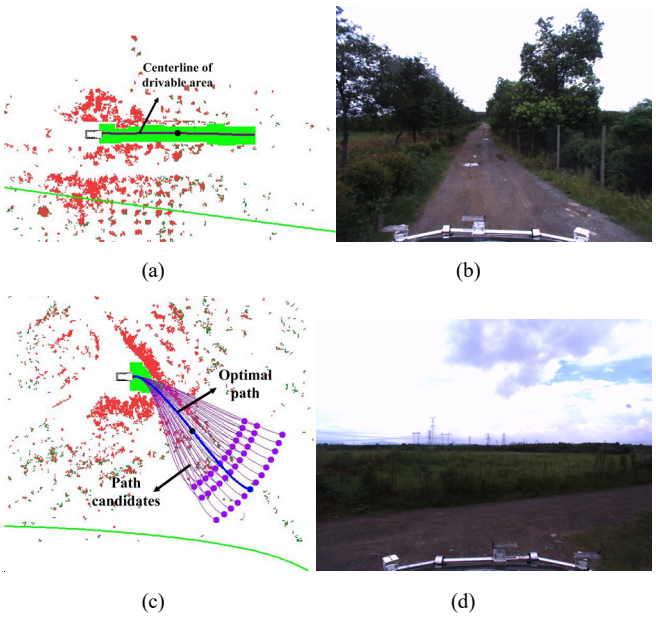

Fig. 12. Correction baseline generation. (a) a snap shot of centerline extraction from drivable area. (b) the image taken by the front camera of the AGV corresponding to (a). (c) a snap shot of the optimal path generation. (d) the image taken by the front camera of the AGV corresponding to (c).

A. Results of correction baseline generation

The proposed correction baseline generation methods are tested in the field test. The baseline generated with centerline extraction and the multi-resolution trajectory planner are shown in Fig. 12. It can be seen from Fig. 12 that the baselines can accurately represent the road geometry.

B. Results of reference correction

The proposed reference path correction methods are tested in the field test. The reference path corrected by offset correction and curvature correction are shown in Fig. 13 and Fig. 14.

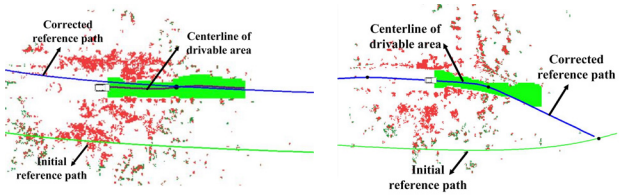

Fig. 13. Reference path corrected by drivable area centerline. (a) offset correction, (b) curvature correction

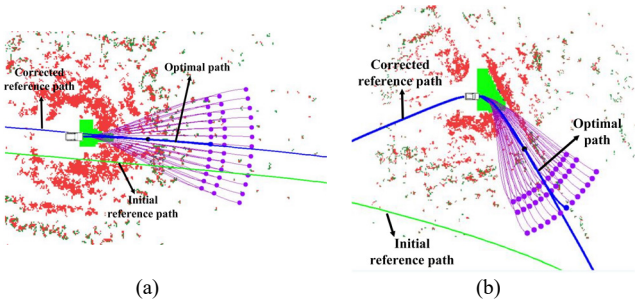

Fig. 14. Reference path corrected by optimal path. (a) offset correction (b) curvature correction

Fig. 15. Correction result

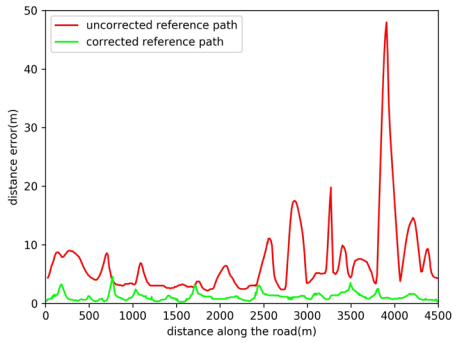

Fig. 16. Corrected reference path

Fig. 13 shows the reference path corrected by offset correction with baseline generated by centerline extraction. Fig. 13(a) shows the reference path corrected by offset correction when the angle θ is less than 10 degree. Fig. 13(b) shows the reference path corrected by curvature correction when the angle θ is greater than 10 degree.

Fig. 14 shows the reference path corrected by offset correction and curvature correction with the optimal path generated by multi-resolution trajectory planner.

The green curve in Fig. 15 shows the reference path that is corrected with the proposed method. The red curve in Fig. 16 represents the distance error, which is defined as the distance from the point road to the closest point on the reference path, between the corrected reference path and the road. The green curve in Fig. 16 represents the distance error between the initial reference path and the road. The maximal distance error in the initial reference path is 50m. With the proposed method, the maximal distance error in the corrected reference path is reduced to 5m.

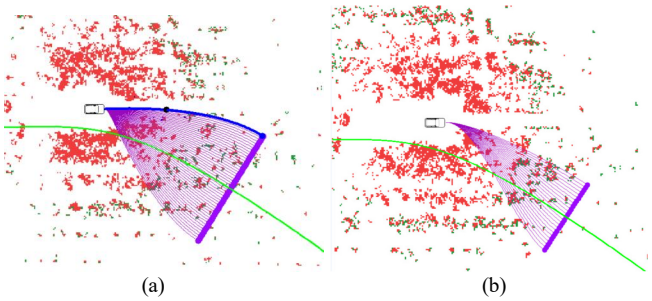

(a) (b)

Fig. 17. Two consecutive results of trajectory planning with uncorrected reference path

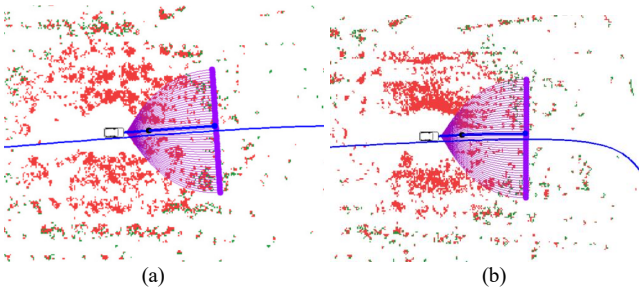

(a) (b)

Fig. 18. Two consecutive results of trajectory planning results with corrected reference path

Fig. 17 shows the results of local trajectory planner using uncorrected initial reference path. The uncorrected reference path contains distance and curvature errors that result in unstable local trajectory planning which may eventually lead to overshoot, oscillation or even require stop-steer-go motions. By correcting reference path, the search space of local trajectory planner is reduced, allowing a more robust and accurate local trajectory planning, as shown in Fig. 18.

V. Conclusion

In this paper, we propose a reference path correction method that can be used in unstructured environments which are difficult to obtain reliable prior information. In order to make the reference path accord with the road geometry, centerline extracted from drivable area and optimal trajectory generated from multi-resolution trajectory planner are used as correction baseline that represents the road geometry. Also, depending on the distance and angle difference between the correction baseline and the initial reference path, offset correction and curvature correction are applied to correct the reference path. The experimental results show that the proposed method can effectively reduce the distance and curvature errors in the reference path, improve the robustness and accuracy of the local trajectory planning in unstructured environments.

References

[1] M. Likhachev and D. Ferguson, "Planning long dynamically feasible maneuvers for autonomous vehicles," *The International Journal of Robotics Research*, vol. 28, no. 8, pp. 933 – 945, 2009.

[2] D. Dolgov, S. Thrun, M. Montemerlo, and J. Diebel, "Path planning for autonomous vehicles in unknown semi-structured environments," *The International Journal of Robotics Research*, vol. 29, no. 5, pp. 485 – 501, 2010.

[3] Y. Kuwata, S. Karaman, J. Teo, E. Frazzoli, J. How, and G. Fiore, "Real-time motion planning with applications to autonomous urban driving," *Control Systems Technology, IEEE Transactions on*, vol. 17, no. 5, pp. 1105 – 1118, 2009.

[4] U. Schwesinger, M. Rufli, P. Furgale, and R. Siegwart, "a sampling based partial motion planning framework for system-compliant navigation along a reference path," in *Intelligent Vehicles Symposium Proceedings*. IEEE, 2013, Conference Paper, pp. 391–396.

[5] X. Li, Z. Sun, A. Kurt, and Q. Zhu, "A sampling-based local trajectory planner for autonomous driving along a reference path," in *Intelligent Vehicles Symposium Proceedings*. IEEE, 2014, Conference Proceedings, pp. 376 – 381.

[6] C. E. Beal and J. C. Gerdes, "Model predictive control for vehicle stabilization at the limits of handling," *Control Systems Technology, IEEE Transactions on*, vol. 21, no. 4, pp. 1258 – 1269, 2013.

[7] X. Li, Z. Sun, Q. Zhu, and D. Liu, "A unified approach to local trajectory planning and control for autonomous driving along a reference path." in *Mechatronics and Automation (ICMA)*, IEEE, 2014, Conference Proceedings, pp. 1716-1721.

[8] Li, Chao, et al. "Reference path optimization for autonomous ground vehicles driving in structured environments." in *Computational Intelligence and Applications (ICCIA)*, IEEE, 2017, Conference Proceedings, pp. 172-176.

[9] J. wung Choi, R. Curry, and G. Elkaim, "Path Planning Based on Bezier Curve for Autonomous Ground Vehicles", *Proc. of 2008 World Congress on Engineering and Computer Science*, pp. 158-166, October, 2008.

[10] Garcia, Olmer, Randerson Lemos, and Janito Vaqueiro Ferreira, "Local and Global Path Generation for Autonomous Vehicles Using Splines," *Ingeniería*, vol. 21, no. 2, pp. 188-200, 2016.

[11] P. A. Theodosis and J. C. Gerdes, "Nonlinear optimization of a racing line for an autonomous racecar using professional driving techniques," in *ASME 2012 Dynamic Systems and Control Conference Joint with the Jsme 2012 Motion and Vibration Conference*, 2012, pp. 235–241.

[12] X. Li, Z. Sun, Z. He, Q. Zhu, and D. Liu, "A practical trajectory planning framework for autonomous ground vehicles driving in urban environments," in *IEEE Intelligent Vehicles Symposium (IV)*, IEEE, 2015, Conference Proceedings, pp. 1160-1166.

[13] M. Werling, S. Kammel, J. Ziegler, and L. Groll, "Optimal trajectories for time-critical street scenarios using discretized terminal manifolds." *The International Journal of Robotics Research* , vol. 31 no. 3, pp. 346-359, Dec. 2011.

[14] Elshamarka, Ibrahim, and Abu Bakar Sayuti Saman. "Design and implementation of a robot for maze-solving using flood-fill algorithm," *International Journal of Computer Applications*, vol.56, no.5, pp. 8-13, 2012.